Published online 14 February 2008 *Nucleic Acids Research, 2008, Vol. 36, No. 6* **1965–1975**
doi:10.1093/nar/gkm1079

Secondary DNA structure formation for *Hoxb9* promoter and identification of its specific binding protein

Takumi Yamagishi[1,2], Shigehisa Hirose[2] and Takashi Kondo[1,*]

[1]Kondo Research Unit, Brain Development Research Group, Brain Science Institute, Institute of Physical and Chemical Research (RIKEN), 2-1 Hirosawa, Wako, Saitama 351-0198 and [2]Department of Biological Sciences, Tokyo Institute of Technology, 4259 Nagatsuta-cho, Midori-ku, Yokohama 226-8501, Japan

Received July 6, 2007; Revised November 12, 2007; Accepted November 15, 2007

ABSTRACT

Hox **genes determine anterior–posterior specificity of an animal body. In mammals, these genes map onto four chromosomal loci in a clustered manner, and their expression is regulated in a coordinated manner according to their chromosomal structure. In the present study, we analysed the *Hoxb9* promoter and found that promoter activity in cultured cells is linked to secondary structure formation of promoter DNA. In nuclear extracts, we also detected binding activity specific for secondary-structured DNA. We successfully isolated a candidate gene encoding this specific DNA-binding protein, FBXL10, and demonstrated the effects of the gene product on *Hoxb9* promoter activity. Our results suggest that DNA can regulate gene expression by other, non-sequence-specific modes of genetic coding.**

INTRODUCTION

Many genes related to developmental processes have temporally and spatially restricted expression profiles that correspond to their roles during the development of multicellular organisms. Failure to regulate a gene often has deleterious consequences that may affect the life of an organism. Although much information exists on transcription regulation, details of regulation mechanisms taking place at the genome level remain elusive. Indeed, it remains a mystery how countless enhancers and promoters interact in an orderly fashion on a single macromolecule of DNA such as a chromosome.

Hox genes encode a group of transcription factors at work during development. These factors are required for anterior–posterior specification of body segments. In mammals, 39 *Hox* genes have been identified, and about 10 of these genes form a gene cluster on the same strand of DNA. These gene clusters map onto four genomic loci called *HoxA*, *B*, *C* and *D* complexes (1,2). These genes show a characteristic genomic organisation in which the order of their chromosomal transcription units mirrors the spatial order of their expression domains along the anterior–posterior axis of the developing embryo. *Hox* genes located at the 3′ extremity of the complex are activated in anterior embryonic domains, whereas genes located at progressively more 5′ positions are transcribed in more posterior areas. This phenomenon, called 'spatial colinearity', was originally described in *Drosophila* and further extended to all bilaterians exhibiting an anterior–posterior axial polarity (3–6). A similar type of colinearity can be observed over time in vertebrates such that *Hox* genes located at the 3′ extremity are activated earliest and genes located at progressively more 5′ positions are transcribed later, according to their order on the genome (7–9). Thus, 'temporal colinearity' is a characteristic of *Hox* gene regulation in vertebrates.

The spatial and temporal regulation of the *Hox* complex has been proposed to be a multi-step process, with each step being initiated by progressive release from heterochromatic silencing (8–10). Although the mechanistic basis of the progressive activation of genes is largely unknown, we have demonstrated that interaction between the 5′-upstream region of the *Hox* complex and promoters of resident *Hox* transcription units are important for early silencing (8,9). To elucidate the mechanisms underlying this higher-order regulatory system, we performed a functional analysis of one key DNA element—the *Hox* promoter. All mammalian *Hox* complexes are known to contain 4th, 9th and 13th paralogous genes. Therefore, we selected the *Hoxb9* promoter as our study system based on an assumption that DNA structures surrounding important regions are better conserved than DNA structures in functionally neutral regions. Here, we report that the functional promoter fragment forms a secondary structure. We subsequently isolated factors that bind this promoter.

*To whom correspondence should be addressed. Tel: +81 48 467 6729; Fax: +81 48 467 6729; Email: TKondo@brain.riken.jp

MATERIALS AND METHODS

Cell cultures and luciferase activity assays

P19 cells were cultured as described previously (11). HeLa cells and NIH3T3 cells were cultured in Dulbecco's Modified Eagle's Medium (Invitrogen) supplemented with 10% heat-inactivated fetal bovine serum (JRH).

Luciferase assays were carried out with the Dual-Luciferase Reporter Assay system (Promega). *Hoxb9* upstream fragments were ligated into a pGL4.12 vector (Promega). Transfection efficiency was monitored using a *Renilla reniformis* luciferase reporter driven by a TK promoter (pGL4.74, Promega). Cells were transfected with constructs and siRNAs using Lipofectamine 2000 (Invitrogen) according to the manufacturer's protocols. Chemiluminescence was measured with a luminometer LB410 (Berthold Technologies, Inc.). Values are presented as means and standard deviations of at least four independent experiments.

RNAi

For RNAi, the siRNAs used were Stealth^{TM} RNAi (Invitrogen) designed according to the manufacturer's protocol. The siRNA sequences against human *FBXL* were as follows:

iRhF10, AAGUAAGUGAGACUGGAUCUCCACC;
iRhF11, UUGGCCACUGUACUAUAGGAACUCC.

To examine the effects of these siRNAs on *Hoxb9* promoter activity, we extracted total RNA from HeLa cells with TRIzol (Invitrogen).

The siRNA sequences against mouse *Fbxl* were as follows:

iRmF10-a, AAGUAAGUGAGACUGGAUCUCCACC;
iRmF10-b, UUCACACUCACUUCUCCGCUUGGCA;
iRmF11, UAUAUUUGUUGGUUUGGAGCUUCUC.

Twenty-four hours after transfecting siRNA into P19 cells, we started retinoic acid (RA) treatment. We isolated RNA 72 h after siRNA transfection (48 h after RA treatment). First-strand cDNA synthesis was carried out using 5 μg of total RNA and SuperScript III First-Strand Synthesis SuperMix (Invitrogen) according to the manufacturer's instructions. We assessed *Hox* and *Fbxl* genes expression in HeLa and P19 cells by real-time PCR (RT–PCR) using a Corbett RG-3000 and Invitrogen Platinum SYBRGreen PCR kit. We calibrated the real-time PCR results by Rotor-Gene 6 Software (Corbett Research) with standard cDNAs whose concentrations are known. We also carried out real-time PCR with β-actin as a control in HeLa and P19 cells.

We used the following primers in which the first letter of each primer—h or m—represent human or mouse, respectively; hm primers are used both for human and mouse.

hβ-actin-F, TGGACATCCGCAAAGACCTG;
hβ-actin-F, ACATCTGCTGGAAGGTGGAC;
mβ-actin-F, CATGTTTGAGACCTTCAACAC;
mβ-actin-R, GTGATGACCTGGCCGTCAGG;
m*Hoxb9*-F, TTTGCGAAGGAAGCGAGGAC;
m*Hoxb9*-R, AAGAGTGAGCTGGGGAAGGG;
hm*Fbxl10*-F, CAAGGAGCAGAAGATGAACCG;
hm*Fbxl10*-R, TGGGGCTTCTCGTATTTCCG;
hm*Fbxl11*-F, ACTGCTGTCGGGTCTTCCACT;
h*FBXL11*-R, CGGTTTCCTGTTGAATCTGGG;
m*Fbxl11*-R, GATTTTCCTGTTCAGTCTGGGC.

Gel mobility shift assay

We performed electrophoretic mobility shift assay (EMSA) as described previously (11). Nuclear extracts were isolated as described previously (12). For competition studies, 12.5-, 25-, 50-, and 100-fold molar ratios of cold DNA against the probe were added.

South-western screening

South-western screening was carried out according to the procedure established by Vinson and colleagues (13), with slight modifications. Instead of using 10^6 c.p.m./ml of probe, we used 10^4 c.p.m./ml of probe in order to facilitate the detection of specific binding to the probe. We isolated 55 clones after screening a P19 cDNA library and selected one clone that displayed fragment A-specific binding, but not fragment B-specific binding, upon further South–western screening.

Antibodies

We generated a polyclonal antibody against FBXL10 by immunizing rabbits with a peptide corresponding to amino acids 923–938 of mouse Fbxl10. Mouse monoclonal antibody (mAb) to ubiquityl-histone H2A and mouse mAb against FLAG were purchased from Upstate and Sigma, respectively.

Chromatin immunoprecipitation (ChIP)

ChIP experiments were performed based on a protocol described previously (9). After P19 cells were cultured with or without 0.3 μM of RA for 48 h in Petri dishes, we collected the cells for ChIP assay. Immunoprecipitation was performed with either anti-Fbxl10 or anti-ubiquityl-histone H2A antibody. To isolate bound chromatin, we used Dynabeads conjugated with Protein A and G for anti-Fbxl10 antibody and Dynabeads rat anti-Mouse IgM for ubiquitylated histone (Dynal Biotech). Samples were washed, reverse crosslinked and digested with proteinase K. Purified DNA samples were analysed by RT–PCR.

RESULTS

Correlation between promoter activity and secondary structure formation of the *Hoxb9* promoter

Transfection assays using P19, HeLa and NIH3T3 cell lines demonstrated that *Hoxb9* promoter activity required a 289-bp fragment that contains the 274-bp fragment upstream of the transcription initiation site (−274 to +15 bp from transcription initiation site; fragment A in Figure 1A and B). Shorter fragments (fragment B, −216 to +15 bp; fragment C, −196 to +15 bp) significantly decreased promoter activity (Figure 1A and B). These results generally agree with those previously reported, except that the differences in promoter activity between

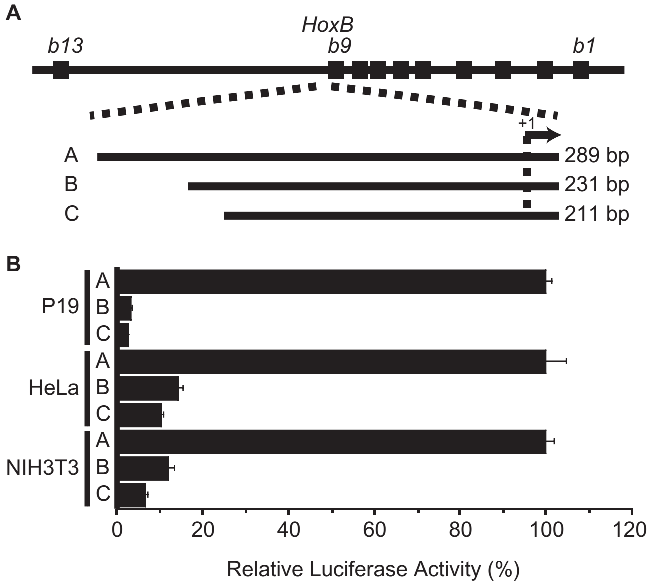

Figure 1. Luciferase assays of *Hoxb9* promoter activity. (**A**) Diagram of DNA fragments used for analysis. The top-most line represents a map of the *HoxB* complex. We assessed the effects of three different fragments (A, B and C) on promoter activity. (**B**) Relative luciferase activities of promoter assay constructs in P19, HeLa and NIH3T3 cells.

fragments A and B were much greater than those we observed previously (11). This is probably because, in the present study, we used a different vector backbone in the luciferase constructs and we used high-turnover luciferase assays to assess promoter activity.

Although the promoter activities of fragments A and B clearly differed, EMSA and footprinting failed to show that nuclear extracts contain binding activity on the DNA spanning from positions −210 to −274 of promoter fragment A (11). Instead, we found that the 296-bp fragment A separated into multiple bands when electrophoresed on native polyacrylamide gels in the absence of protein, while fragments B and C did not separate into distinct multiple bands, suggesting that fragment A becomes highly structured (Figure 2A), perhaps attaining a secondary structure. We confirmed by sequencing that the multiple bands from fragment A share the same sequence. This structural change may be responsible for altering its mobility on EMSA gels. Similarly sized DNA fragments, including fragments from λ-phage and mammalian DNA such as those from the human c-*myc* promoter, did not show similar heterogeneous mobility patterns in native gels. Among the multiple bands derived from fragment A, the mobility of the fastest-moving band corresponded to the mobility of a same-sized linear DNA fragment (289 bp). To get insight into the secondary structure of the slower-moving band, we conducted digestion experiments with S1 nuclease and mung bean nuclease, which enabled us to identify single-stranded residues within the DNA fragment. The slower-moving bands were much more sensitive to these nucleases than the fastest-moving band (linear DNA fragment). These results indicate that the slower-moving band contains single-stranded residues. We could not detect, however, signs of digestion at specific residues. The fragment represented by the slow-moving band may contain multiple sites that are sensitive to S1 nuclease digestion. Alternatively, the strands close to the ends of this fragment may have dissociated.

Although the detailed secondary structure of the *Hoxb9* promoter fragment (fragment A) is yet to be determined, we do know that this fragment contains a GC-rich region, which is a prime candidate for triplex DNA formation. To take on a triplex structure, however, this short DNA fragment must be circular, not linear, in order to attain the torsion needed for triplex formation; thus, the secondary structure of this fragment is unlikely to be triplex (14). Nevertheless, the link we observed between secondary structure formation and promoter activity suggests that secondary structure formation confers promoter activity to the *Hoxb9* fragment.

To examine secondary structure formation of the *Hoxb9* promoter in another species and to confirm the importance of secondary structure formation, we also isolated the corresponding fragment from the human genome. The human counterpart of this fragment derived from the *HOXB9* promoter showed about 92% sequence identity to the fragment derived from the Mm*Hoxb9* promoter (Supplementary Figure S1A) and exhibited more promoter activity than the mouse promoter (data not shown). Moreover, we also observed that the Hs*HOXB9* promoter fragment underwent secondary structure formation similar to that as the Mm*Hoxb9* promoter fragment (Supplementary Figure S1B). These results indicate that the characteristic ability to undergo secondary structure formation is conserved over species.

Specific binding activity against secondary structured *Hoxb9* promoter in nuclear extracts

EMSA performed in the presence of nuclear extracts from P19 and HeLa cells revealed that these extracts had specific binding activity for the slow-moving band of fragment A (Figure 2B). Although the slow-moving band (arrows in Figure 2) disappeared when binding activity was assessed in the presence of nuclear extracts (Figure 2B), the fast-moving band (asterisks in Figure 2) was unaffected (Figure 2B). These findings indicate that binding activity was structure specific rather than sequence specific, as the DNA represented by the fast-moving and slow-moving bands shared identical sequences. Although the addition of nuclear extracts completely abolished the slow-moving band, no distinct new bands were formed, suggesting that the DNA–protein complex contained multiple proteins. To confirm whether the binding activity was specific, we performed competition assays using as competitors fragment A (which forms the secondary structure) and fragment B (which showed much less secondary structure formation) (Figure 2B). Adding fragment A to the assay mixture caused the slow-moving band (indicated by arrow in the Figure 2B) to reappear, suggesting that DNA–protein complex is dissociated by competition. On the other hand, adding fragment B did not cause the slow-moving band to reappear (Figure 2B). Taken together, these findings

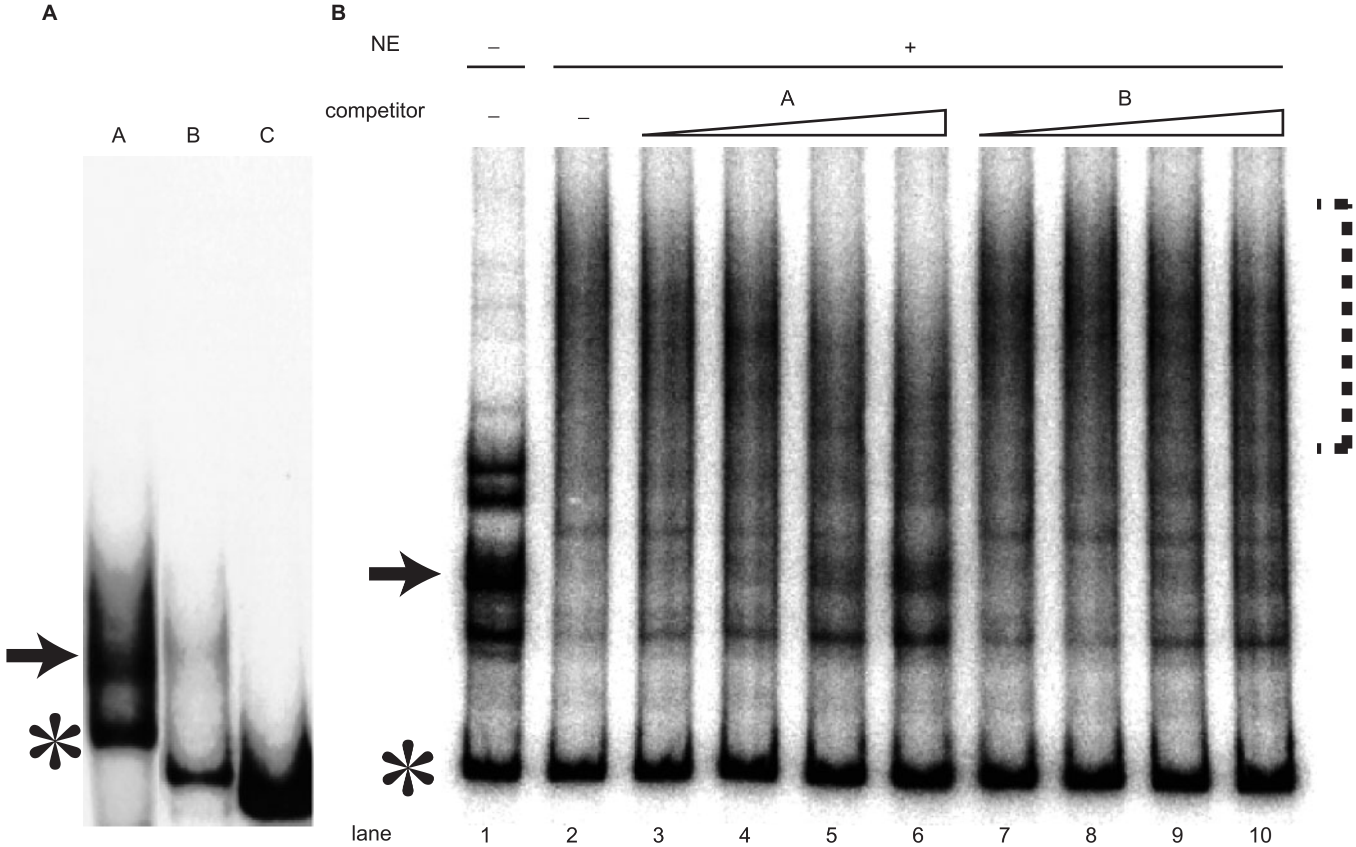

Figure 2. *Hoxb9* promoter fragment forms a secondary structure. (**A**) Native gel electrophoresis of fragments A, B and C revealed that only the fragment having promoter activity, fragment A, separated into multiple, but discrete, bands. Bands consisting of slow-moving secondary-structured DNA are indicated by arrows, and bands consisting of fast-moving linear DNA are indicated by asterisks. (**B**) EMSA performed in the absence (–) or presence (+) of nuclear extracts (NE) from P19 cells and competition assay for protein–DNA binding. Because a protein in the NE specifically binds the highly structured DNA fragment (indicated by arrow), the slow-moving band disappeared and formed a smear (indicated by dotted line) in the presence of NE, as shown in lanes 1 and 2. Lanes 3–10 show results from competition assays. The concentrations of competitor DNA used were 12.5-, 25-, 50- and 100-fold molar ratio relative to the probe (lanes 3 and 7; 4 and8; 5 and 9; 6 and 10, respectively). Adding fragment A as a competitor caused the band (arrow) to reappear (lanes 3–6). Fragment B as a competitor, however, was much less effective in causing the band to reappear, indicating that fragment B failed to compete successfully.

indicate that (i) fragment A, which functions as a promoter, is capable of taking on a secondary structure; and (ii) protein(s) in the nuclear extracts specifically bind the secondary-structured fragment A.

Cloning of secondary-structured DNA-specific binding protein

To determine the significance of these findings, we attempted to clone the secondary structured DNA-specific binding protein(s). We isolated a clone after screening a P19 cDNA library using the South–western method (Figure 3A) (13) and verified its binding activity further using EMSA (Figure 3B). Database searches revealed that the clone is identical to *Fbxl10*, human PCCX2, DKFZp434I0535 and JEMMA. *Fbxl10* encodes an F-box, a motif for E3 ubiquitin ligase (15). It also encodes a bipartite nuclear localization signal (NLS) as well as leucine-rich domains (Figure 3A). The presence of cxxc and PHD-finger domains suggests that FBXL10 may be related to chromatin modification factors such as those encoded by *Polycomb*-group (*PcG*) and *trithorax*-group (*trxG*) genes. Recently, FBXL10 was identified as the histone demethylase, JHDM1b, and several following works reported that the jmjC domain is responsible for histone demethylation activity (16–19). Thus, the presence of a jmjC domain in *Fbxl10* further supports the idea that *Fbxl10* participates in chromatin modification.

Another *Fbxl10* homologue, *Fbxl11* (known as JHDM1a), shares high homology with all the functional domains of *Fbxl10*.

We fused in-frame the part of *Fbxl10* containing the cxxc and PHD finger domains with GST (heavy line in Figure 3A), and subjected the resulting fusion protein to EMSA. As with EMSA performed in the presence of nuclear extracts, EMSA with the GST-fusion protein resulted in a band shift similar to that of the slow-moving band of fragment A (Figure 3B), however, without yielding new discrete bands, only a smear. These findings suggest that a homo–multimer complex formed around the GST–*Fbxl10* fusion protein. Moreover, fragment A not B, successfully out-competed binding to the GST-fusion protein as observed in the EMSA experiments performed with nuclear extracts (Figure 3B). From these

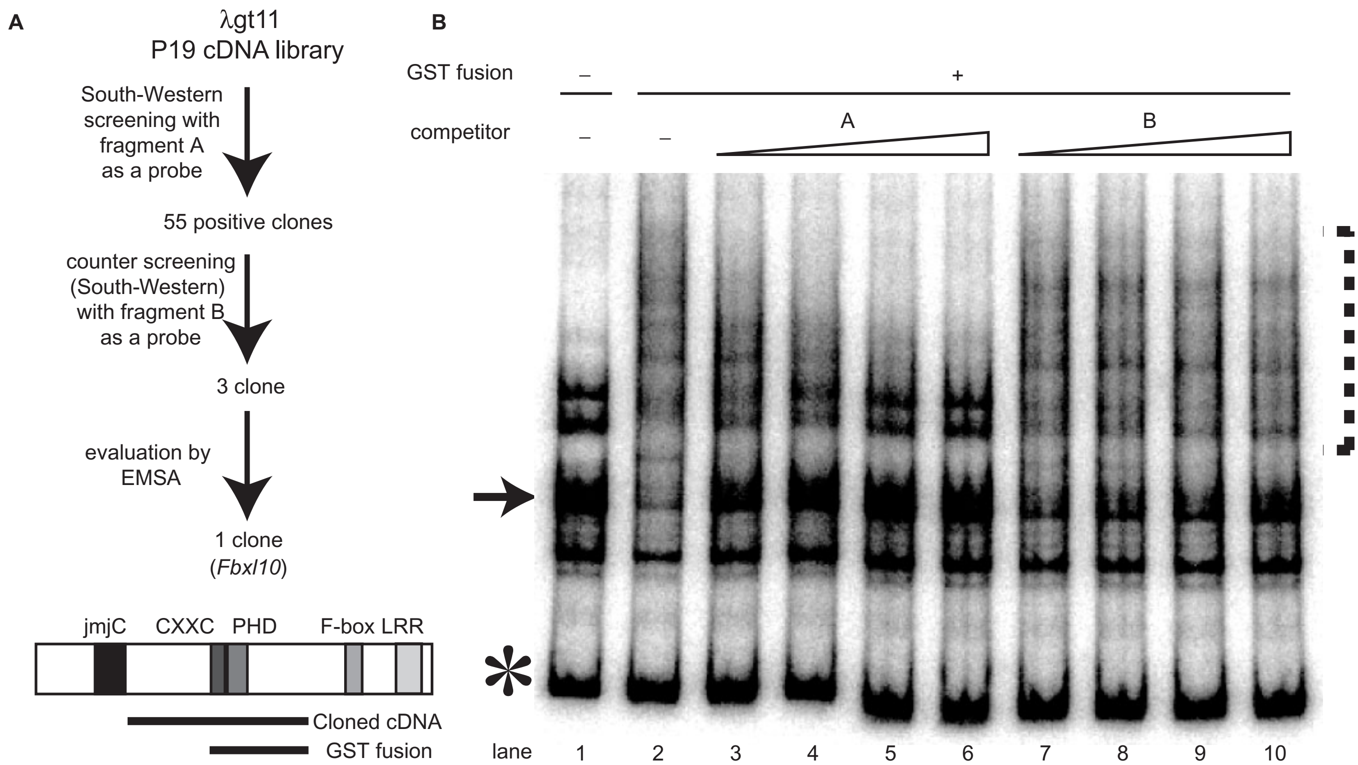

Figure 3. Cloning of *Fbxl10*, which encodes a protein that binds the highly structured *Hoxb9* promoter fragment. (**A**) Scheme of cloning strategy and schematic diagram of the obtained *Fbxl10* gene. Cloning was done by using South–western methods and fragment A as a probe. The 55 clones we isolated were counter-selected by South–western methods and fragment B as a probe. Further confirmation was carried out with EMSA. We obtained the partial sequence of *Fbxl10* through South–western cloning. Sequence analysis of full-length *Fbxl10* cDNA revealed several motifs: jmjC, cxxc, Zn-finger, PHD Zn-finger and F-box domains and leucine-rich repeats (LRR). (**B**) EMSA with GST-fusion protein derived from the cloned fragment. The fragment used to produce the GST-fusion protein is indicated as a bold black line located below *Fbxl10* (panel A). Competition assays were carried out as described in the legend of Figure 2. As observed with our EMSA analyses performed with nuclear extracts (NE) (see Figure 2), fragment A competed successfully for binding, while fragment B did not. Arrow points to the slow-moving band; asterisk marks the band representing linear DNA.

experiments, we concluded that *Fbxl10* is likely to be the DNA-binding protein within the nuclear extracts that specifically bound the secondary-structured fragment A.

Effect of secondary-structured DNA-specific binding protein on *Hoxb9* promoter activity

We performed a functional analysis of *Fbxl10* and *Fbxl11* using the RNAi gene-knockdown technique. We designed siRNAs against human *FBXL10* (iRhF10 siRNAs) and *FBXL11* (iRhF11 siRNAs) and examined the influence of these siRNAs on *Hoxb9* promoter activity by co-transfecting them into HeLa cells with luciferase constructs containing fragment A. Transfection of *FBXL10* and *FBXL11* siRNAs reduced intrinsic *FBXL10* and *FBXL11* expression (Figure 4). We observed cross-repression of *FBXL10* and *FBXL11* by these siRNAs. The siRNA iRhF10 effectively reduced *FBXL10* and *FBXL11* mRNA expression (Figure 4). Although iRhF11 effectively down-regulated *FBXL11*, it had a relatively weak effect on *FBXL10*. Luciferase activity of the reporter construct containing fragment A showed 2.8-fold up-regulation compared to that of the control when HeLa cells were co-transfected with the reporter construct and iRhF10 (Figure 4). In contrast, luciferase activity did not change significantly when HeLa cells were co-transfected with the construct and iRhF11 (Figure 4). These results suggest that *Fbxl10* is the primary factor that influences *Hoxb9* promoter activity. We could not exclude, however, the influence of *Fbxl11* on *Hoxb9* promoter activity.

We further examined the effects of *Fbxl10* and *Fbxl11* genes on the native *Hox* locus using P19 embryonal carcinoma (EC) cell cultures. Although undifferentiated P19 cells showed little or no expression of *Hoxb9* gene, P19 EC cells express *Hoxb9* gene when differentiation is induced by RA treatment (11). To determine how *Fbxl10* and *Fbxl11* genes affect the regulation of native *Hoxb9* gene, we knocked down either *Fbxl10* or *Fbxl11* expression in RA-treated P19 cells with siRNA and measured *Hoxb9* gene expression by RT–PCR (Figure 5). Forty-eight hours after RA induction, a time at which *Hoxb9* gene is expressed (Figure 5) (11), *Hoxb9* exhibited elevated expression when *Fbxl10* expression was suppressed by treatment with *Fbxl10*-specific siRNA (iRmF10-a or iRmF10-b) (Figure 5). Despite having a high degree of sequence homology with *Fbxl10*, *Fbxl11* in general did not influence *Hoxb9* expression (Figure 5; iRmF11). These results support our hypothesis that *Fbxl10* interacts with the *Hoxb9* promoter whereas *Fbxl11* does not, even

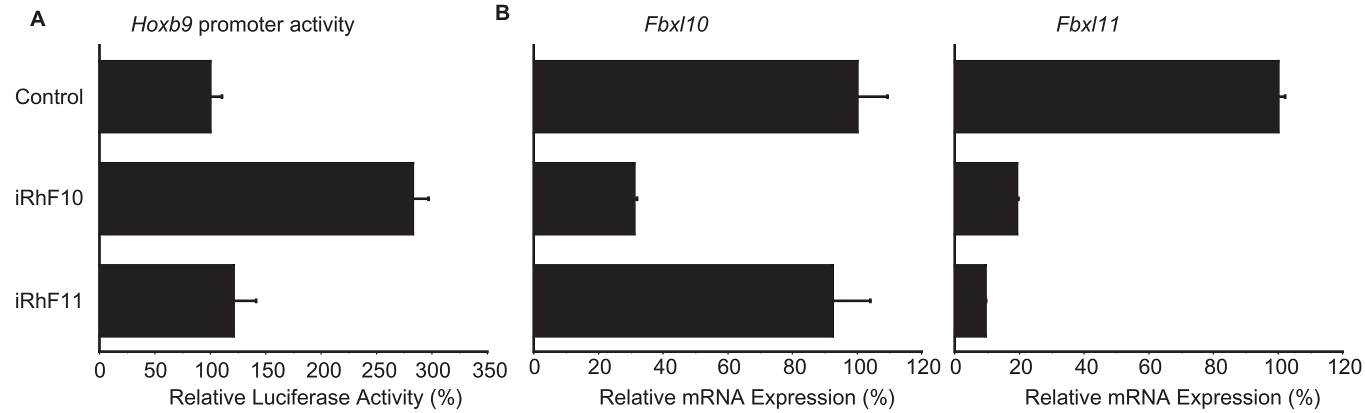

Figure 4. Effects of *FBXL* genes on *Hoxb9* promoter activity in HeLa cells. (**A**) Effects of siRNAs on *FBXL* expression. We designed siRNAs—iRhF10 and iRhF11—and used RT–PCR to examine the effects of these siRNAs on *Hoxb9* promoter activity. Specific siRNAs against *FBXL10* increased promoter activity, whereas siRNAs specifically against *FBXL11* either did not increase or weakly increased promoter activity. (**B**) Treatment with siRNAs influences intrinsic *FBXL* expression. Each of these siRNAs down-regulated *FBXL* expression, as evident by the definitive reduction of RT–PCR signals. RT–PCR samples were normalized relative to β-actin expression.

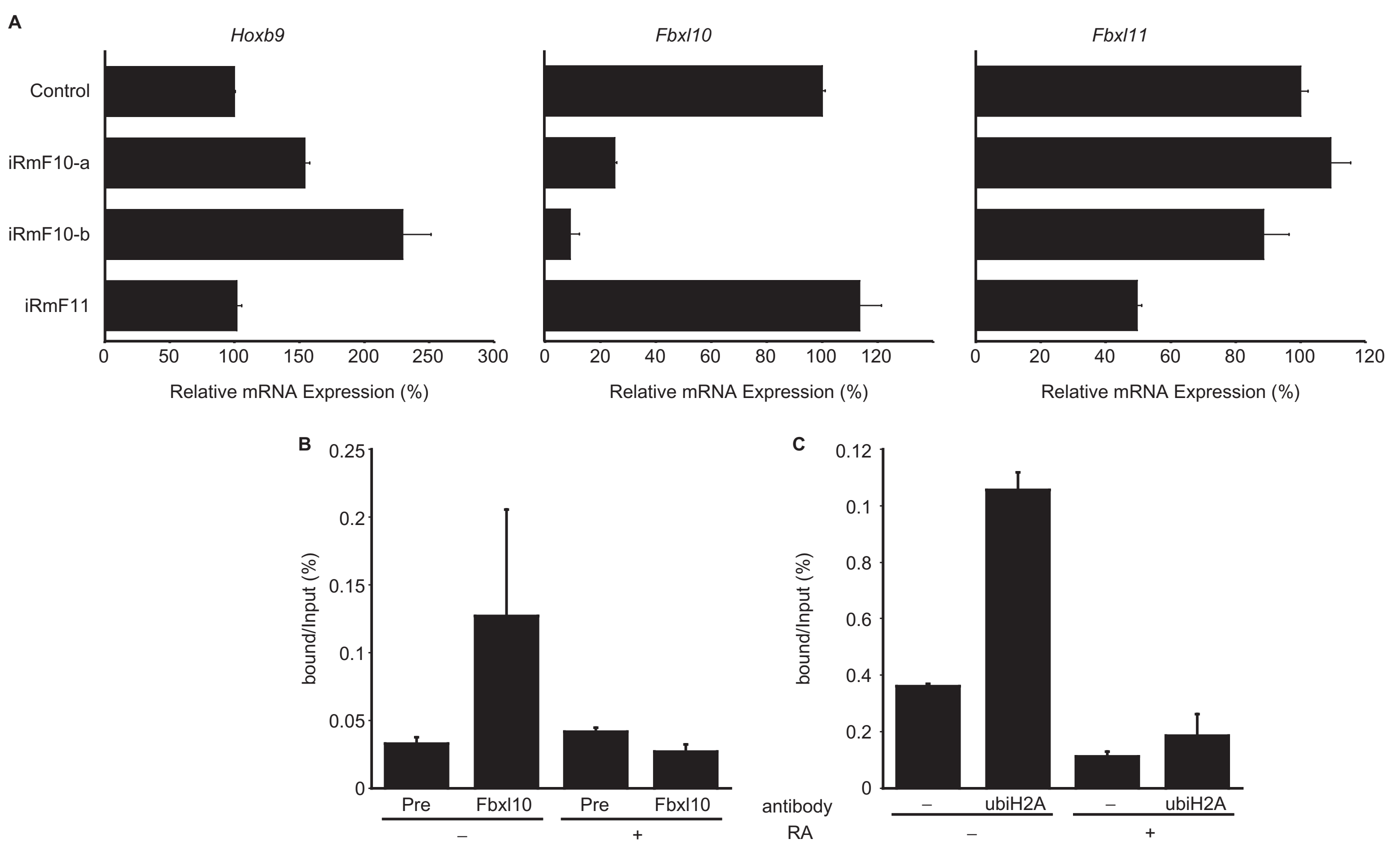

Figure 5. Influence of *Fbxl* genes on the native *Hoxb9* induction system. (**A**) The influences of *Fbxl* genes were analysed by introducing siRNAs. We designed three siRNAs—iRmF10-a, iRmF10-b and iRmF11—and used RT–PCR to examine the effects of these siRNAs on intrinsic *Hoxb9* and *Fbxl* expression. The siRNAs were introduced into P19 cells during the 24-h pre-incubation period and during the 48-h RA-induction period (total exposure time: 72 h). RT–PCR samples were normalized relative to β-actin expression. Transfection of *Fbxl10*-specific siRNAs elevated *Hoxb9* expression (left graph), whereas transfection of *Fbxl11*-specific siRNAs did not significantly influence *Hoxb9* expression. The specificity of these siRNAs on target genes is shown in the remaining graphs as indicated. (**B**) Binding of FBXL10 protein to native *Hoxb9* promoter in P19 cells. ChIP analysis revealed that FBXL10 binds *Hoxb9* promoter in undifferentiated P19 cells but not in differentiated P19 cells, which express *Hoxb9*. (**C**) Histone H2A ubiquitylation status of the *Hoxb9* promoter differs as P19 cells differentiate. ChIP was carried out with anti-ubiquitylated histone H2A antibody. Similar to the profile observed for FBXL10, ubiquitylated histone H2A seems to accumulate at the *Hoxb9* promoter region when P19 cells are in an undifferentiated state.

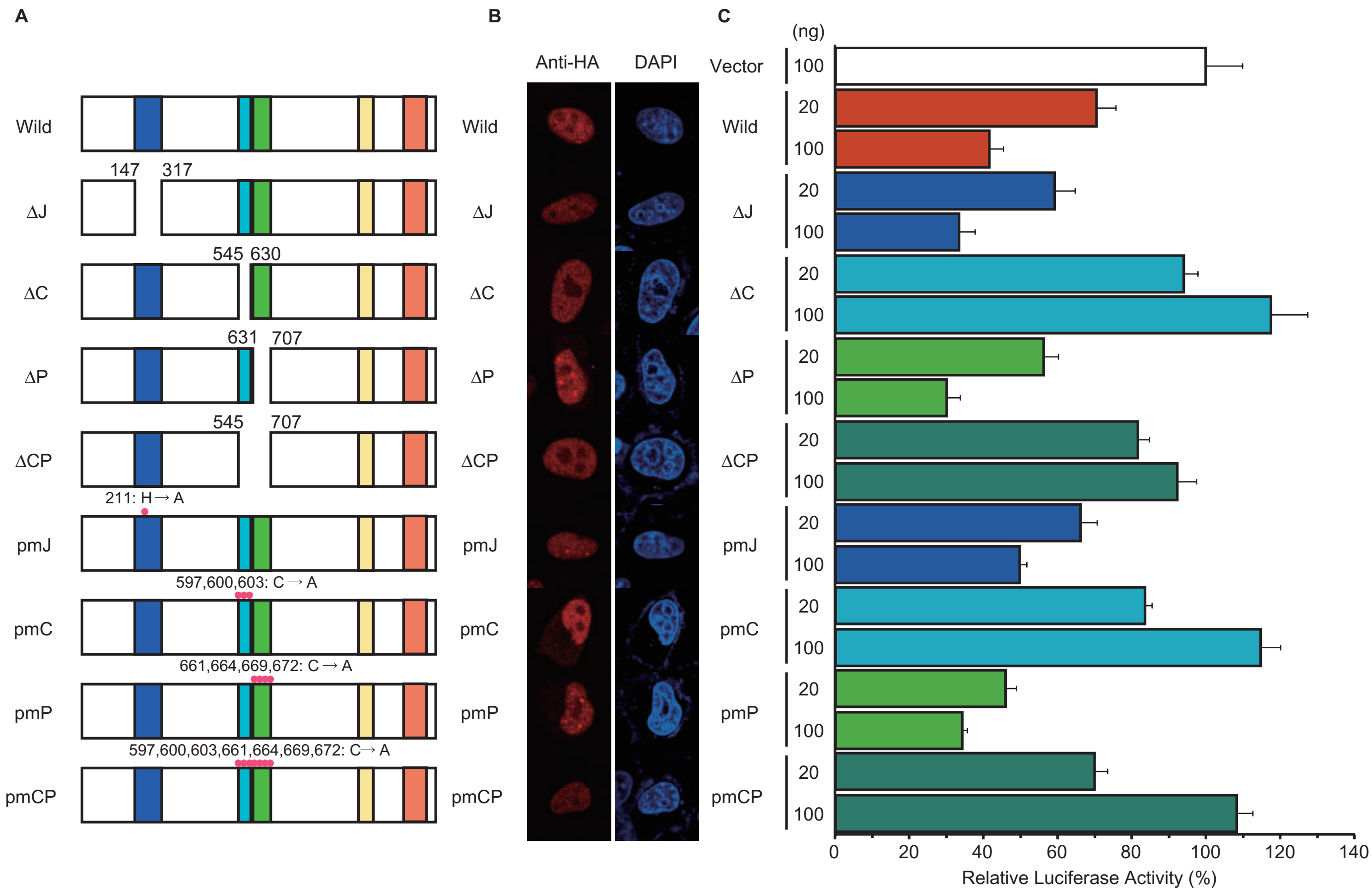

Figure 6. Assessment of domains involved in the specific regulation of *Hoxb9*. (**A**) Schematic diagrams of *Fbxl10* mutants. ΔJ, C and ΔP represent deletion mutants of the jmjC domain, cxxc domain, and the PHD domain, respectively. ΔCP represents a deletion mutant of both cxxc and PHD domains. Three other mutants, pmJ, pmC, pmP and pmCP, have point mutations in jmjC, cxxc, PHD and both the cxxc and PHD domains, respectively. (**B**) Subcellular localization of *jcp1* mutants. Each mutant protein was fused with an HA-tag at C-terminal and then expressed in HeLa cells. Fusion proteins were localized by immunocytochemistry with anti-HA antibody. All mutants localized to the nucleus. (**C**) Effect of *jcp1* mutants on *Hoxb9* promoter activity. We co-transfected HeLa cells with mutant-expressing plasmids and *Hoxb9* luciferase reporter plasmids and examined the influence of each mutation by measuring luciferase activity.

though the structures of their protein products resemble each other.

To examine the direct interaction between FBXL10 protein and the *Hoxb9* promoter, we performed ChIP assays using anti-FBXL10 antibody (Figure 5B). However, we observed FBXL10 binding onto the *Hoxb9* promoter in undifferentiated P19 cells. FBXL10 binding to the *Hoxb9* promoter disappeared in differentiated P19 cells, which express *Hoxb9*. These results correspond well to our siRNA findings showing *Fbxl10* repression activity on the *Hoxb9* promoter and strongly suggest that *Fbxl10* is indeed a *Hox* regulator. To further investigate mechanisms underlying the regulation of *Hoxb9* gene expression during differentiation, we conducted ChIP assays using various anti-histone antibodies. While we did not detect differences in ChIP assays performed with anti-K9 acetylated histone H3, anti-K36 trimethylated histone H3, anti-K36 dimethylated histone H3 and anti-K36 monomethylated histone H3 antibodies, we did detect reduced binding to the *Hoxb9* promoter when ChIP was performed with anti-ubiquitylated histone H2A antibody (Figure 5C). This reduced binding of ubi-H2A was similar to the reduced binding of FBXL10 we observed in differentiated P19 cells (Figure 5B). These observations suggest the possibility that *Fbxl10* functions as a histone ubiquitylase not a histone demethylase during *Hox* regulation.

Analysis of *Fbxl10* domains required for regulation of *Hoxb9* gene

To determine the importance of the cxxc and PHD domains, which we used to make fusion proteins for DNA-binding assays (Figure 3), we created several mutants of *Fbxl10* having either deletion or point mutations in the jmjC domain, cxxc domain and/or the PHD domain (Figure 6A). All of these mutant proteins localized to the nucleus, as did wild-type *Fbxl10* (Figure 6B). Next, to observe how these mutants influence promoter activity, we introduced the constructs expressing these mutants into HeLa cells along with a luciferase reporter construct driven by *Hoxb9* promoter fragment A.

Elevated expression of wild-type *Fbxl10* down-regulated luciferase activity (Figure 6C). Luciferase activity remained unaffected in cells transfected with the vector construct (negative control) (Figure 6C). Both deletion and point mutants of the cxxc domain (ΔC, ΔCP, pmC and pmCP in Figure 6) failed to affect luciferase activity, whereas the mutants of the jmjC or PHD domains influenced luciferase activity in a manner similar to wild-type *Fbxl10*. Thus, the repressive activity of *Fbxl10* was completely abolished by mutations within the cxxc domain, but mutations in the jmjC and PHD domains did not influence the activity of *Fbxl10* in this assay system. We observed a similar effect of *Fbxl10* on human *HOXB9* promoter and similar loss of *Fbxl10* repressive activity resulting from point mutations in the cxxc domain (Supplementary Figure 1C). Although we could not demonstrate the importance of the jmjC and PHD domains, these results indicated that the cxxc domain plays a critical role in *Fbxl10*-mediated regulation of *Hoxb9*.

The secondary structure formation of other *Hox* promoters

We expected that secondary structure formation was not restricted to the *Hoxb9* promoter; thus, we extensively searched for other promoters within the *Hox* complex capable of taking on secondary structures. We isolated several DNA fragments containing the sequences surrounding predicted transcription initiation sites of several *Hox* genes and briefly analysed the promoter activity of these fragments by measuring luciferase activity (Figure 7A and B). We identified several potential *Hox* promoter fragments having lengths of about 300–700 bp (Figure 7B). These fragments clearly displayed promoter activity when compared to that of the control luciferase vector lacking a promoter, although most of these promoters showed weaker activity than the *Hoxb9* promoter (Figure 7B). Some of these fragments with promoter activity, such as *Hoxd1* and *Hoxd8*, also showed heterogeneous mobility in native gels, as observed with *Hoxb9* promoter fragment A (Figure 7C), although some fragments from *Hoxa1*, *Hoxa13* and *Hoxb4* did not. At the very least, these results suggest that promoter regions of some *Hox* genes also have the potential to take on secondary structures, as with the case of *Hoxb9*. As we observed with *Hoxb9*, overexpression of *Fbxl10* also influenced the promoter activities of *Hoxd1* and *Hoxd8* (Figure 7D). In contrast, promoter fragments that did not take on secondary structures, such as *Hoxa1*, *Hoxa13* and *Hoxb4*, did not influence promoter activity (Figure 7D). Overexpression of *Fbxl10* activated the *Hoxd1* promoter but repressed *Hoxb9* and *Hoxd8* promoters (Figure 7D). Although we clearly observed a correlation between secondary structure formation of *Hox* promoters and *Fbxl10*, these results suggest that the *Hox* promoter response to *Fbxl10* varies.

DISCUSSION

Secondary structure formation of *Hox* promoters

We have previously proposed that multiple DNA–site interactions are important for the coordinated expression of *Hox* genes (8–10,20). This hypothesis also posited a crucial role of regulated positional movement of chromosomal loci in this *Hox* gene system. Recent reports have emphasized the significance of chromosomal position within the nucleus during various biological processes (21,22). Chambeyron and colleagues (23,24) demonstrated the importance of chromosomal positioning of *Hox* genes during development, correlating chromosomal position with transcription activity. In this scheme, DNA–DNA interactions (direct or indirect via protein–protein interactions) can crucially determine the relative position of DNA loci.

The mechanisms underlying chromosomal movement remain completely unknown. However, it is clear that the interaction between the repressive region (8) and promoters of resident *Hox* genes are decisive factors in this regulatory process. Here, we focused on the *Hoxb9* promoter and found a novel characteristic of *Hox* promoter DNA—the *Hox* promoter forms secondary structures. Although, the relationship between this phenomenon, chromosomal movement and the formation of secondary DNA structures remains to be determined, our results suggest that the secondary structure formation of promoter DNA is important for *Hox* gene regulation. Indeed, we observed that several DNA fragments from *Hox* complexes displayed a similar heterogeneity in mobility when assessed in native gels, but DNA fragments from non-*Hox* regions or other organisms, such as bacteria, did not display this mobility shift (data not shown). The nature of the higher structures formed by various *Hox* promoter fragments remains elusive. However, it is doubtful that these structures represent DNA triplets, since the secondary structure of the short DNA fragments we analysed was stable and detectable by native gel electrophoresis. Even the linear form of this fragment lacked the torsion derived from circular forms of DNA, which is required for triplet formation (14). We believe that the formation of secondary structures may be a novel type of genetic coding, although secondary structure formation to some degree is dependent on DNA sequence.

Secondary-structured DNA-specific binding protein and gene transcription

Isolation of a clone (*Fbxl10*) encoding a protein that specifically bound to a secondary-structured *Hox* promoter fragment and determination of its influence on *Hox* promoter activity shed light onto the significant role of secondary structures of promoter DNA in transcription regulation. Furthermore, promoter analysis using other *Hox* promoters indicated that *Fbxl10* regulates multiple *Hox* genes not just *Hoxb9* gene. The molecular structure of this protein suggests that it is a chromatin factor, having shared homology with the cxxc and PHD Zn-finger domains of *PcG* and *trxG* genes. The *Fbxl10* and *Fbxl11* genes also contain sequences encoding an F-box domain, a protein motif found in a component of E3 ubiquitin ligase, strongly suggesting that *Fbxl10* and *Fbxl11* proteins participate in protein ubiquitylation processes. Recently, histone ubiquitylation has been shown to be important in histone modifications involved in transcription

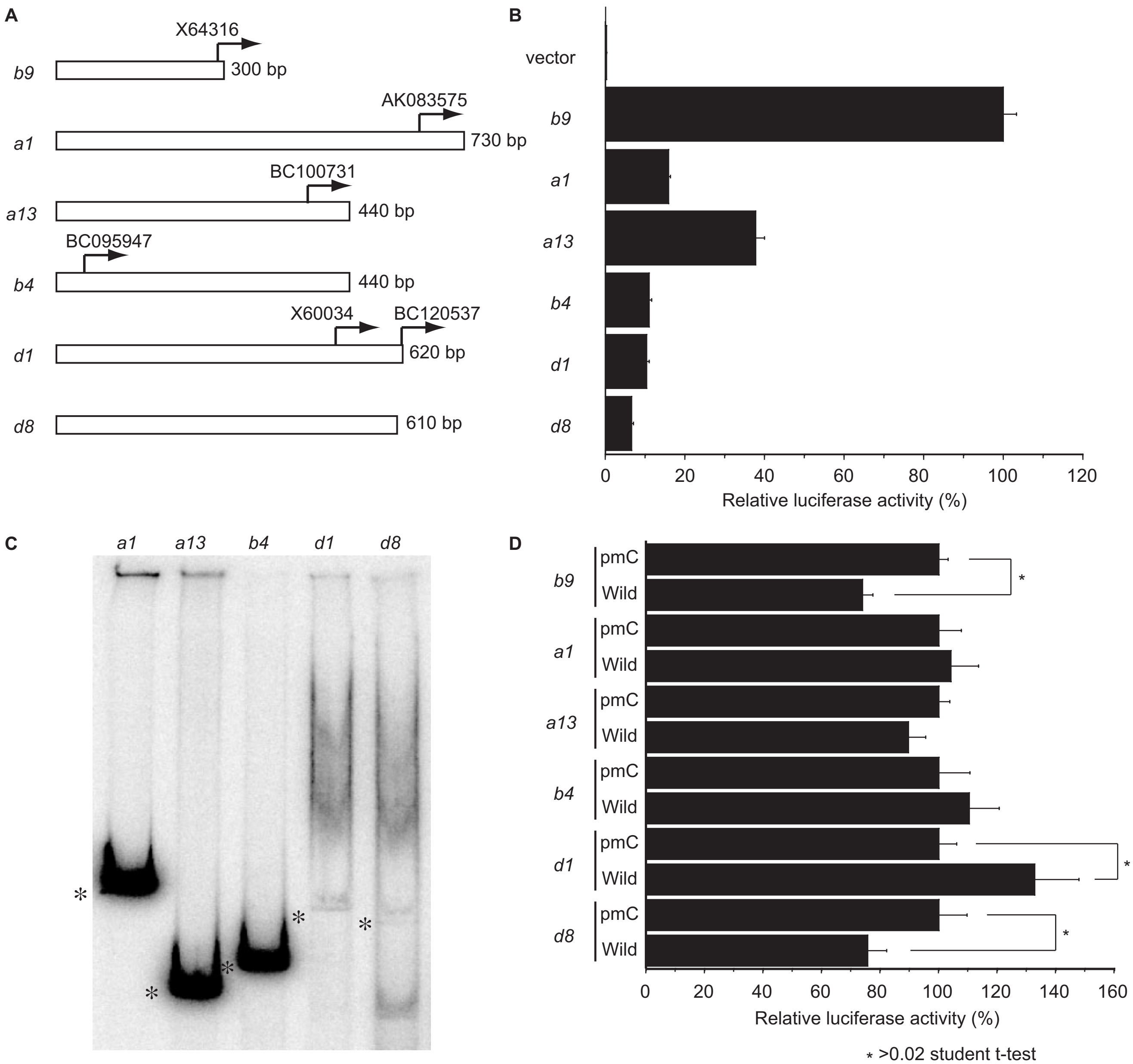

Figure 7. Higher structure formation of *Hox* promoters. (**A**) Examples of isolated *Hox* promoter fragments. Arrows indicate the 5′ end of cDNA sequences annotated in the NCBI sequence library. The transcription initiation site of *Hoxb9* was determined previously (11). (**B**) Relative luciferase activity of isolated promoter fragments. The promoter intensities of these fragments are shown relative to the luciferase activity measured in cells transfected with *Hoxb9* constructs, which was set to 100. The negative control (luciferase vector lacking a promoter fragment) did not show any traces of activity. (**C**) Native gel electrophoresis of *Hox* promoter fragments. The fragments from *Hoxa1*, *Hoxa13* and *Hoxb4* did not exhibit multiple bands, while the fragments from *Hoxd1* and *Hoxd8* separated into multiple bands, as observed with *Hoxb9* (Figure 2). Asterisks mark linear portions of the DNA fragments. (**D**) Effects of *Fbxl10* on *Hox* promoters. Each luciferase construct was co-transfected with an *Fbxl10* expression construct. Co-transfection experiments with the pmC construct represented control experiments (Figure 5). Overexpression of wild-type *Fbxl10* influenced luciferase activity in cells co-transfected with either *Hoxd1* or *Hoxd8* promoter fragments, fragments that take on a higher structure like *Hoxb9*. By contrast, wild-type *Fbxl10* and pmC *Fbxl10* failed to significantly influence luciferase activity in cells co-transfected with *Hoxa1*, *Hoxa13* or *Hoxb4* promoter fragments. Asterisks indicate significant differences compared to cells expressing the control vector according to the Student's *t*-test ($P < 0.03$).

regulation (25). Indeed, Gearhart and colleagues (26) suggested that FBXL10/JHDM1b is a component of the BCOR (BCL6 corepressor) complex and is responsible for histone H2A monoubiquitylation. In addition to these motifs, *Fbxl10* contains a leucine-rich repeat, indicating that it may also interact with other proteins.

The presence of a jmjC domain in *Fbxl10* further supports the idea that it is involved in chromatin modification. Recently, Tsukada and colleagues (16) reported that JHDM1a (*Fbxl11* in the present work) functions as a histone demethylase and that the jmjC domain is responsible for histone demethylation activity.

It is probable, therefore, that *Fbxl10* (also known as JHDM1b) also has histone demethylase activity, since *Fbxl10* and *Fbxl11* (JHDM1a) share high homology throughout their molecular structures, including in their jmjC histone demethylase domains (16). It is also probable that *Fbxl10* is involved in transcription activation processes (16). The coexistence of demethylation activity and ubiquitylation activity in one molecule, *Fbxl10*, is somewhat controversial. Indeed, our analysis of the *Hoxd1* and *Hoxb9* promoters suggests that *Fbxl10* can function differentially to activate or repress promoter activity depending on the promoter or context. Multiple domains of *Fbxl10* and *Fbxl11* proteins may be involved in facilitating the protein–DNA or protein–protein interactions required for complex transcription regulation.

High homology in the molecular structures of *Fbxl10* and *Fbxl11* suggests that the products of these genes may have functional similarities. However, *Fbxl11* did not significantly influence *Hoxb9* regulation in our transient promoter assays or in our assessment of the transcription profile of the native *Hoxb9* gene in P19 EC cells. These results suggest that, despite their high homology, *Fbxl10* and *Fbxl11* differ in their abilities to regulate downstream genes.

The structural composition of *Fbxl10* and *Fbxl11* proteins (e.g. numerous domains for interacting with other proteins) and the complexity of their activity on transcription suggest that *Fbxl10* and *Fbxl11* proteins may function as a structural 'hub' for a multi-protein–DNA complex, and that they may also serve as a functional 'hub', coordinating different functional protein complexes for regulating gene transcription.

With regard to *Hoxb9* transcription, in the present study *Fbxl10* likely functioned as a histone ubiquitylase rather than a demethylase, because ChIP analysis showed that ubiquitylated histone H2A differentially bound the *Hoxb9* promoter, a situation that reflects *Hoxb9* expression during P19 EC cell differentiation. However, we also observed that trichostatin A and butyrate abolished *Fbxl10*-mediated repression of *Hoxb9* promoter, suggesting that HDAC (histone deacetylase) is also involved in *Hox* regulation, as shown in the recently reported case of c-*jun* (27). Recently, other jmjC proteins (Utx and JMJD3) were identified as demethylase *Hox* regulators of K27 trimethylated histone H3 (28,29). According to these schemes, at least three different histone modification activities may intersect through *Fbxl10*. To fully understand the regulatory role of *Fbxl10*, we need to continue to analyse the regulatory mechanisms of *Fbxl10* on *Hox* genes.

Based on the present results, we propose an alternative type of information coding in chromosomal DNA, one that is based on secondary structure rather than on sequence. Although the structure of DNA depends to some degree on nucleotide sequence, we do not yet have sufficient information to correlate sequence with structure. However, the presence of proteins that specifically bind secondary DNA structures and the potential role of these proteins in gene transcription provide further support for the importance of secondary structure formation in DNA.

ACKNOWLEDGEMENTS

We thank T. Kojima and T. Tabata for sharing information and helpful discussions and members of the Kondo laboratory for sharing resources. We also thank M. Ota and Y. Zhang for reading the manuscript. T.K. also thanks D. Duboule and M. Muramatsu for continuous encouragement. This work is supported by a grant from the Human Frontier Scientific Program Organization grant RGY0316/2001-M to T.K. Funding to pay the Open Access publication charges for this article was provided by institutional budget from RIKEN BSI.

Conflict of interest statement. None declared.

REFERENCES

1. Duboule,D. (1994) *Guidebook to the Homeobox Genes*. Oxford University Press, Oxford.
2. Krumlauf,R. (1994) *Hox* genes in vertebrate development. *Cell*, **78**, 191–200.
3. Lewis,E. (1978) A gene complex controlling segmentation in *Drosophila*. *Nature*, **276**, 565–570.
4. Akam,M.E. (1989) *Hox* and *HOM:* Homologous gene clusters in insects and vertebrates. *Cell*, **57**, 347–349.
5. Duboule,D. and Dollé,P. (1989) The structural and functional organization of the murine *HOX* gene family resembles that of *Drosophila* homeotic genes. *EMBO J.*, **8**, 1497–1505.
6. Graham,A., Papalopulu,N. and Krumlauf,R. (1989) The murine and *Drosophila* homeobox gene complexes have common features of organization and expression. *Cell*, **57**, 367–378.
7. Izpisúa-Belmonte,J.-C., Falkenstein,H., Dollé,P., Renucci,A. and Duboule,D. (1991) Murine genes related to the *Drosophila AbdB* homeotic gene are sequentially expressed during development of the posterior part of the body. *EMBO J.*, **10**, 2279–2289.
8. Kondo,T. and Duboule,D. (1999) Breaking colinearity in the mouse *HoxD* complex. *Cell*, **97**, 407–417.
9. Mishra,R.K., Yamagishi,T., Vasanthi,D., Ohtsuka,C. and Kondo,T. (2007) Involvement of *Polycomb*-group genes in establishing *HoxD* temporal colinearity. *Genesis*, **45**, 570–576.
10. Kondo,T., Zákány,J. and Duboule,D. (1998) Control of colinearity in *AbdB* genes of the mouse *HoxD* complex. *Mol. Cell*, **1**, 289–300.
11. Kondo,T., Takahashi,N. and Muramatsu,M. (1992) The regulation of the murine *Hox-2.5* gene expression during cell differentiation. *Nucleic Acids Res.*, **20**, 5729–5735.
12. Dignam,J.D., Lebovitz,R.M. and Roeder,R.G. (1983) Accurate transcription initiation by RNA polymerase II in a soluble extract from isolated mammalian nuclei. *Nucleic Acids Res.*, **11**, 1475–1489.
13. Vinson,C.R., LaMarco,K.L., Johnson,P.F., Landschulz,W.H. and McKnight,S.L. (1988) *In situ* detection of sequence-specific DNA binding activity specified by a recombinant bacteriophage. *Genes Dev.*, **2**, 801–806.
14. Kohwi-Shigematsu,T. and Kohwi,Y. (1991) Detection of triple-helix related structures adopted by poly(dG)-poly(dC) sequences in supercoiled plasmid DNA. *Nucleic Acids Res.*, **19**, 4267–4271.
15. Jin,J., Cardozo,T., Lovering,R.C., Elledge,S.J., Pagano,M. and Harper,J.W. (2004) Systematic analysis and nomenclature of mammalian F-box proteins. *Genes Dev.*, **18**, 2573–2580.

16. Tsukada,Y., Fang,J., Erdjument-Bromage,H., Warren,M.E., Borchers,C.H., Tempst,P. and Zhang,Y. (2006) Histone demethylation by a family of JmjC domain-containing proteins. *Nature*, **439**, 811–816.
17. Whetstine,J.R., Nottke,A., Lan,F., Huarte,M., Smolikov,S., Chen,Z., Spooner,E., Li,E., Zhang,G. *et al*. (2006) Reversal of histone lysine trimethylation by the JMJD2 family of histone demethylases. *Cell*, **125**, 467–481.
18. Yamane,K., Toumazou,C., Tsukada,Y., Erdjument-Bromage,H., Tempst,P., Wong,J. and Zhang,Y. (2006) JHDM2A, a JmjC-containing H3K9 demethylase, facilitates transcription activation by androgen receptor. *Cell*, **125**, 483–495.
19. Klose,R.J., Kallin,E.M. and Zhang,Y. (2006) JmjC-domain-containing proteins and histone demethylation. *Nat*. *Rev*. *Genet*., **7**, 715–727.
20. Yamagishi,T., Ozawa,M., Ohtsuka,C., Ohyama-Goto,R. and Kondo,T. (2007) *Evx2-Hoxd13* intergenic region restricts enhancer association to *Hoxd13* promoter. *PLoS ONE*, **2**, e175.
21. Spilianakis,C.G., Lalioti,M.D., Town,T., Lee,G.R. and Flavell,R.A. (2005) Interchromosomal associations between alternatively expressed loci. *Nature*, **435**, 637–645.
22. Tanemura,K., Ogura,A., Cheong,C., Gotoh,H., Matsumoto,K., Sato,E., Hayashi,Y., Lee,H.W. and Kondo,T. (2005) Dynamic rearrangement of telomeres during spermatogenesis in mice. *Dev*. *Biol*., **281**, 196–207.
23. Chambeyron,S. and Bickmore,W.A. (2004) Chromatin decondensation and nuclear reorganization of the *HoxB* locus upon induction of transcription. *Genes Dev*., **18**, 1119–1130.
24. Chambeyron,S., DaSilva,N.R., Lawson,K.A. and Bickmore,W.A. (2005) Nuclear re-organisation of the *Hoxb* complex during mouse embryonic development. *Development*, **132**, 2215–2223.
25. Wang,H., Wang,L., Erdjument-Bromage,H., Vidal,M., Tempst,P., Jones,R.S. and Zhang,Y. (2004) Role of histone H2A ubiquitination in Polycomb silencing. *Nature*, **431**, 873–878.
26. Gearhart,M.D., Corcoran,C.M., Wamstad,J.A. and Bardwell,V.J. (2006) Polycomb group and SCF ubiquitin ligases are found in a novel BCOR complex that is recruited to BCL6 targets. *Mol*. *Cell*. *Biol*., **26**, 6880–6889.
27. Koyama-Nasu,R., David,G. and Tanese,N. (2007) The F-box protein Fbl10 is a novel transcriptional repressor of c-Jun. *Nat*. *Cell Biol*., **9**, 1074–1080.
28. Lan,F., BaylissP.E., Rinn,J.L., Whetstine,J.R., Wang,J.K., Chen,S., Iwase,S., Alpatov,R., Issaeva,I. *et al*. (2007) A histone H3 lysine 27 demethylase regulates animal posterior development. *Nature*, **449**, 689–694.
29. Agger,K., Cloos,P.A.C., Christensen,J., Pasini,D., Rose,S., Rappsilber,J., Issaeva,I., Canaani,E., Salcini,A.E. *et al*. (2007) UTX and JMJD3 are histone H3K27 demethylases involved in HOX gene regulation and development. *Nature*, **449**, 731–734.